

R. Middei,

S. Bianchi, M. Cappi, P-O. Petrucci, F. Ursini, N. Arav, E. Behar, G. Branduardi-Raymont, E. Costantini, B. De Marco, L. Di Gesu, J. Ebrero, J. Kaastra, S. Kaspi, G. A. Kriss, M. Mehdipour, S. Paltani, U. Peretz, G. Ponti

NGC 7469 ID



> $z=0.016268$
> Seyfert 1 Galaxy
> Flux 0.3-10 keV $\approx 6 \times 10^{-11} \text{ erg cm}^{-2} \text{ s}^{-1}$
> $M \sim 7 \times 10^7 M_{\odot}$
> $L_{\text{Bol}} \sim 10^{45} \text{ erg s}^{-1}$
(Springob et. all. 2005)

Abstract:

We conducted a multiwavelength six-months campaign to observe the nearby Seyfert galaxy NGC 7469 using several observatories. We report the results of the spectral analysis of the 7 simultaneous XMM-Newton and NuSTAR observations. The source shows a remarkable flux variability during the 7 observations, both in the soft and the hard X-ray bands, while the hardness ratios do not show strong variability. The smallest variability timescale is only a few ks. Both phenomenological and physically motivated models are used to describe the broad-band (UV/hard X-ray) spectrum of this rich data-set. We derive physical and geometrical constraints on the inner engine and the circumnuclear matter in NGC 7469 by combining the spectral and variability results obtained.

Observations log

Obs. Satellites	Obs. ID	Star time
XMM-Newton	0760350201	2015-06-12
Nustar	60101001002	2015-06-12
XMM-Newton	0760350301	2015-11-24
Nustar	60101001004	2015-11-24
XMM-Newton	0760350401	2015-12-15
Nustar	60101001006	2015-12-15
XMM-Newton	0760350501	2015-12-23
Nustar	60101001008	2015-12-22
XMM-Newton	0760350601	2015-12-24
Nustar	60101001010	2015-12-25
XMM-Newton	0760350701	2015-12-26
Nustar	60101001012	2015-12-27
XMM-Newton	0760350801	2015-12-28
Nustar	60101001014	2015-12-28

XMM-Newton spectra and timing analysis

Timing analysis (Fig. 1) reveals that NGC 7469 displays a larger amount of variability on the few ks time scales, while among the observations less dramatic flux variations are observed. The higher energy band seems to be constant but the hardness ratios do not show remarkable variations.

XMM-Newton spectra are shown in Fig. 2.

A strong soft excess is present, thus, as a first step, we analyse these spectra above 4 keV. The model we adopt to fit to the data accounts for the continuum emission, a reflected component and two Gaussian lines i.e. the FeK α and FeL γ .

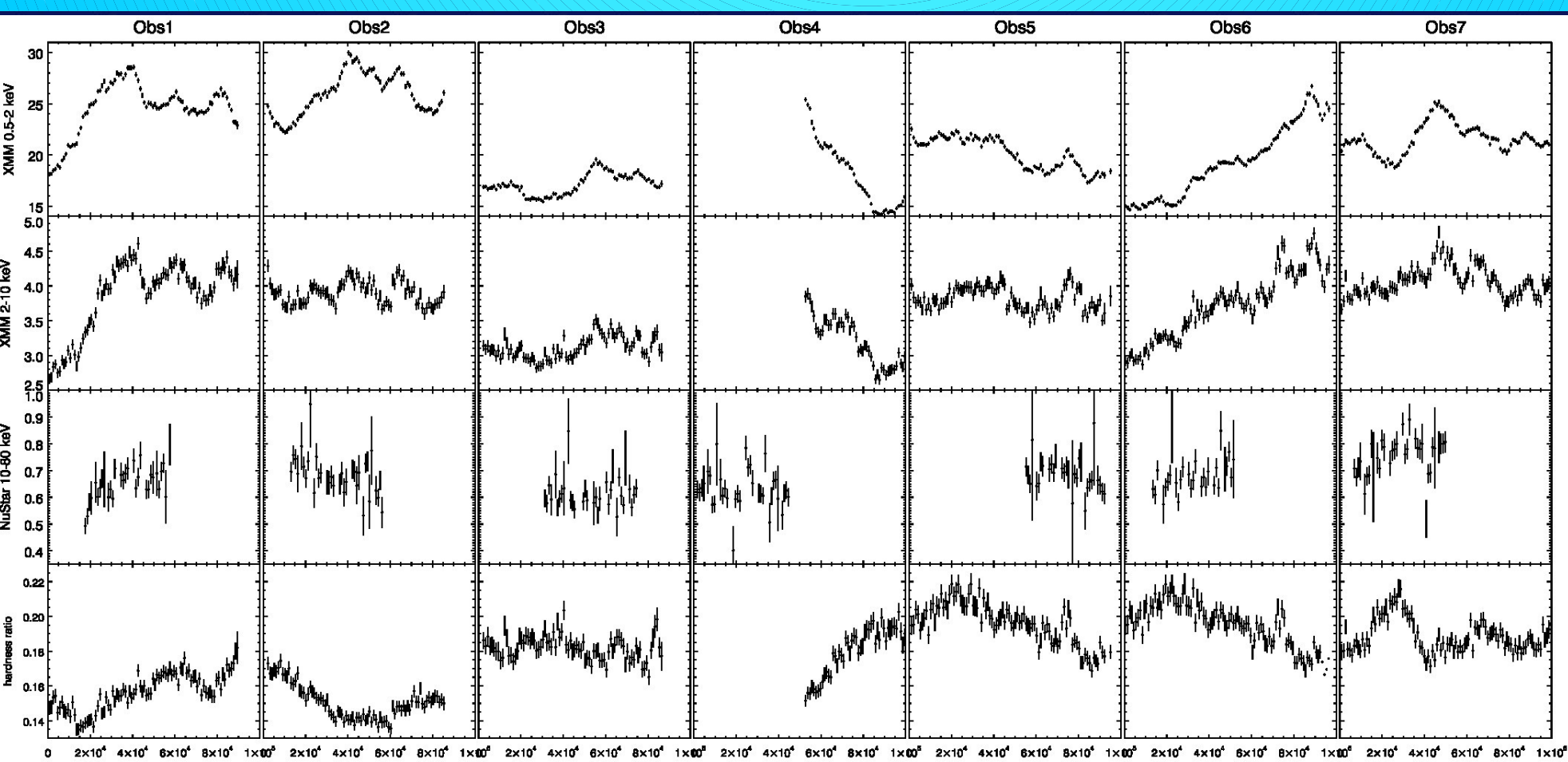


Fig. 1. light curves in the 0.3-2 keV, 2-10 keV, 10-80 keV and hardness ratios (0.3-2/2-10).

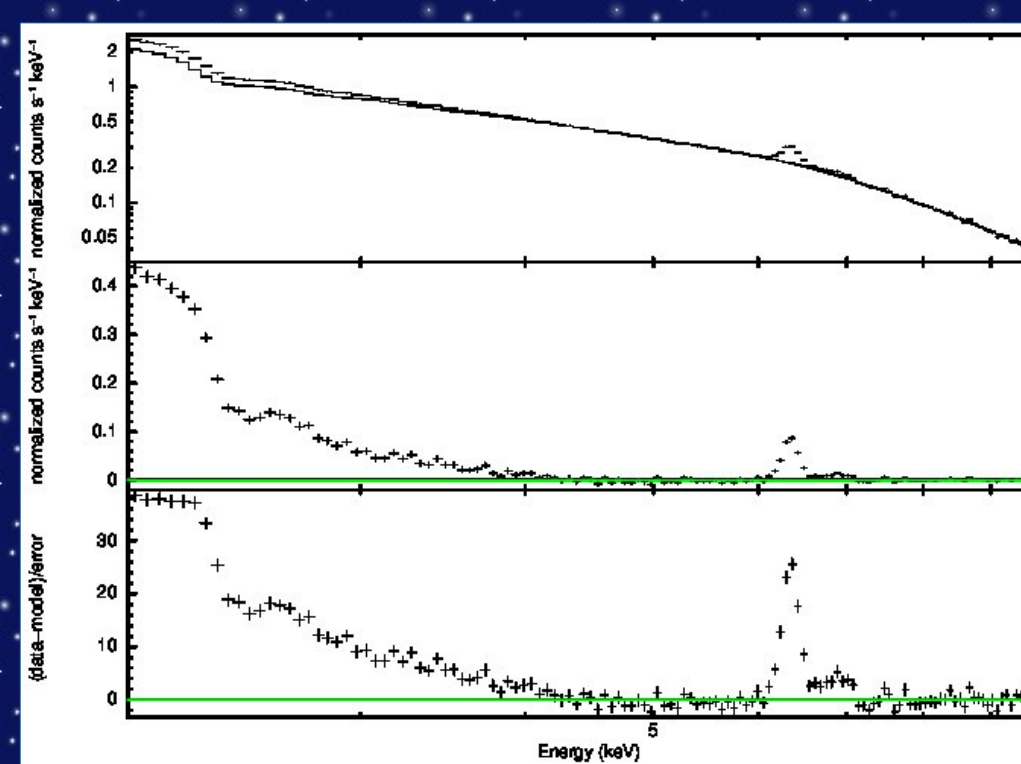


Fig. 2. A simple power law is used to fit the data. The figure shows a strong soft-excess extending up to 4 keV.

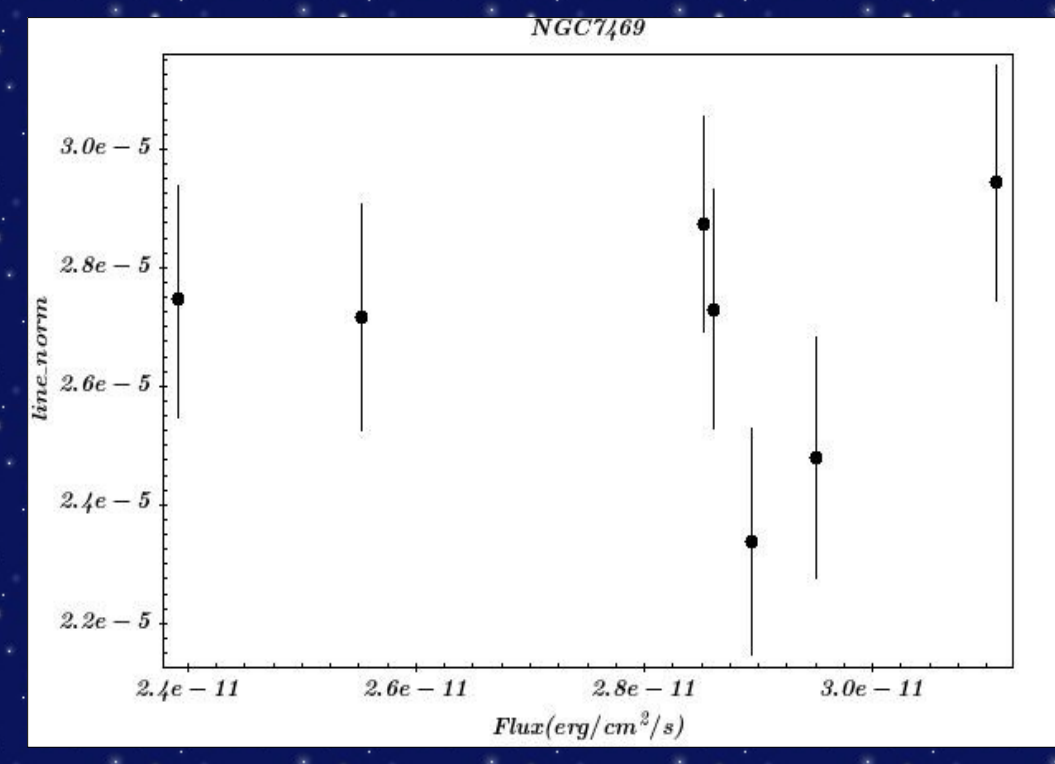


Fig. 3. The neutral iron line flux v.s. the flux for the 7 observations. Errors account for 1 σ uncertainty.

The FeK α

The neutral iron line is constant among the observations and no evidence for relativistic broadening is found. On average the EW=90 eV

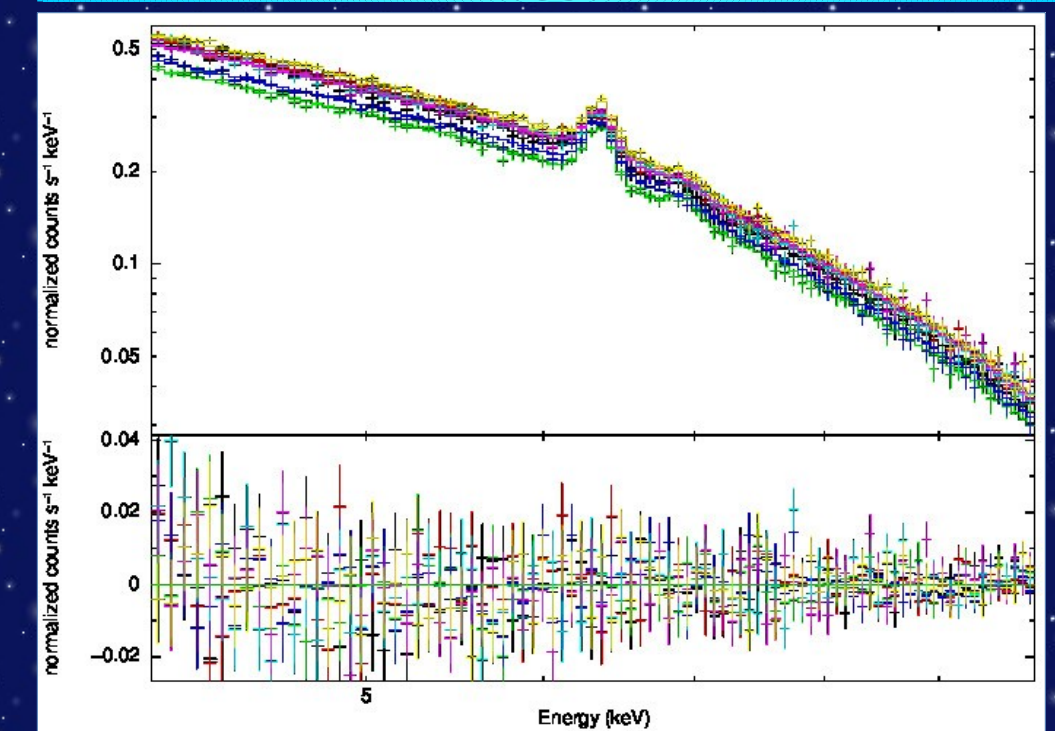


Fig. 2. The best fit to the points X/d.o.f.=1.04 is performed in the 4-10 keV band.

XMM-Newton & NuSTAR analysis

From the XMM-Newton best fit we find no evidence of relativistic effects on the neutral iron line, thus to fit the broad band spectra we adopt a consistent reflection model producing the hump and the narrow line at 6.40 keV, the narrow ionized iron line at 6.966 keV and a high energy cut off.

The best fit we obtain is reported in Fig. 5.

The iron abundance is tied among all the observations, while all the other parameters are free to vary even if they are tied for XMM-Newton and NuSTAR within the same observation.

We report only the gamma values obtained from NuSTAR (on average = 0.17 with respect to XMM, due to known inter-calibration issues (e.g. Cappi et al. 2016)).

From the best fit we study as a function of the 4-78 keV flux the properties of the photon index, the high energy cut-off and the reflection for these spectra, see Fig. 6, Fig. 7 and Fig. 8 respectively.

In all the figures error bars account for 1 σ uncertainty.

The photon index and the high energy cut-off do not vary while a small trend in the reflection fraction is found.

This is consistent with a scenario where all the variability is driven by the normalization of the primary continuum, while the reflection components (including the iron line) are produced by distant material.

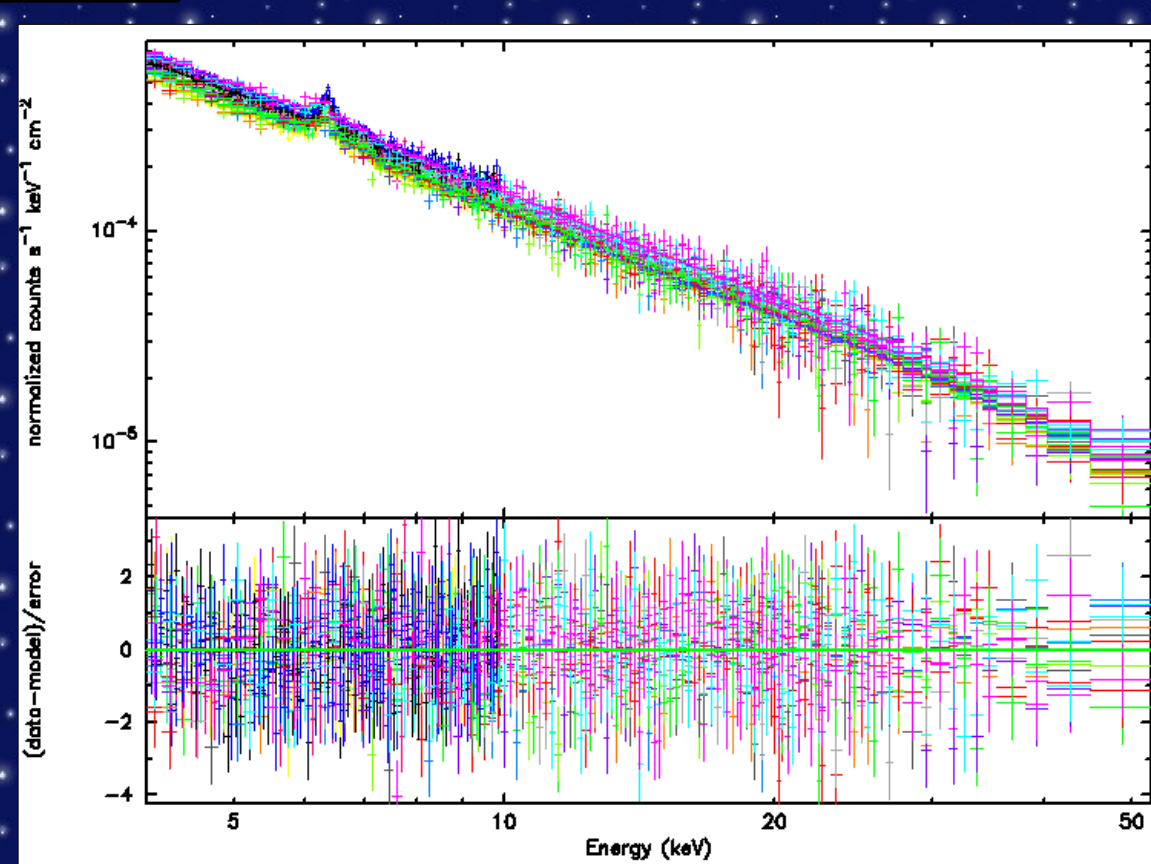


Fig. 5. The best fit to the XMM-Newton and NuSTAR data. X/d.o.f.=1.06

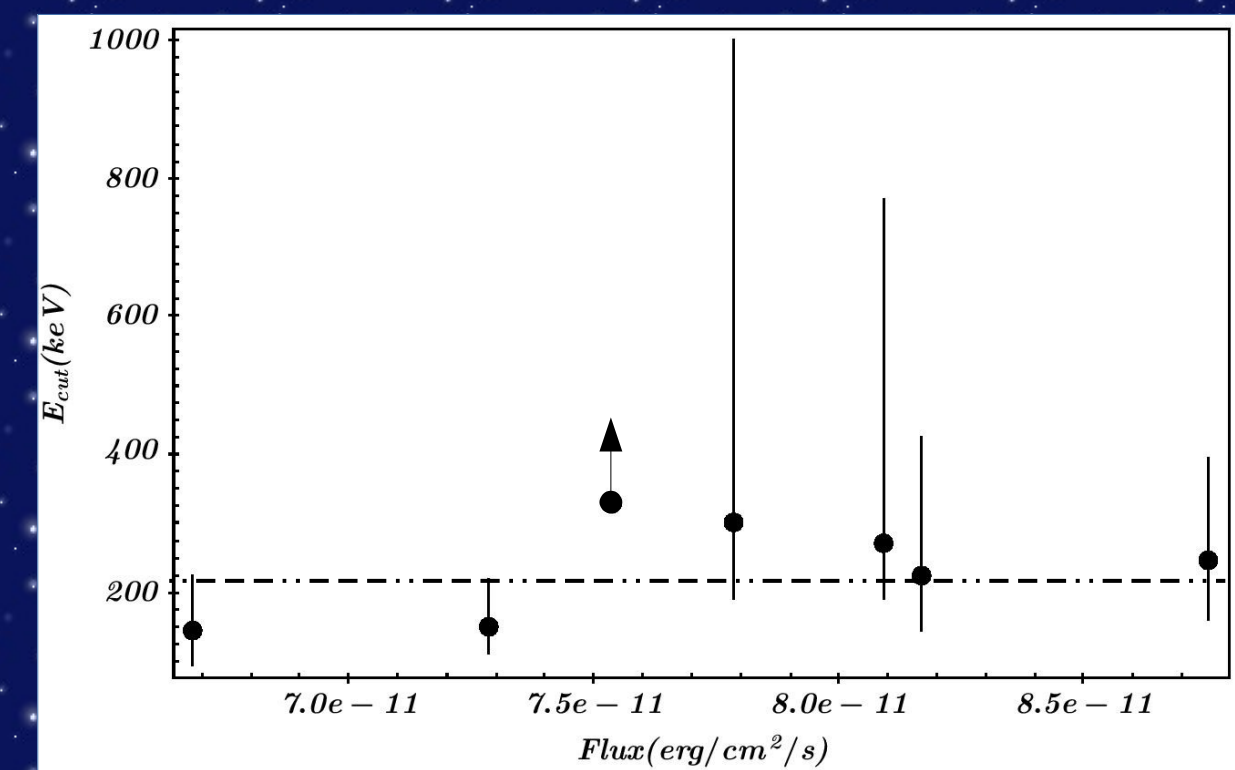


Fig. 7. High energy cut off versus the flux of NGC 7469. The average value $E_{\text{cut-off}} \approx 220$ eV

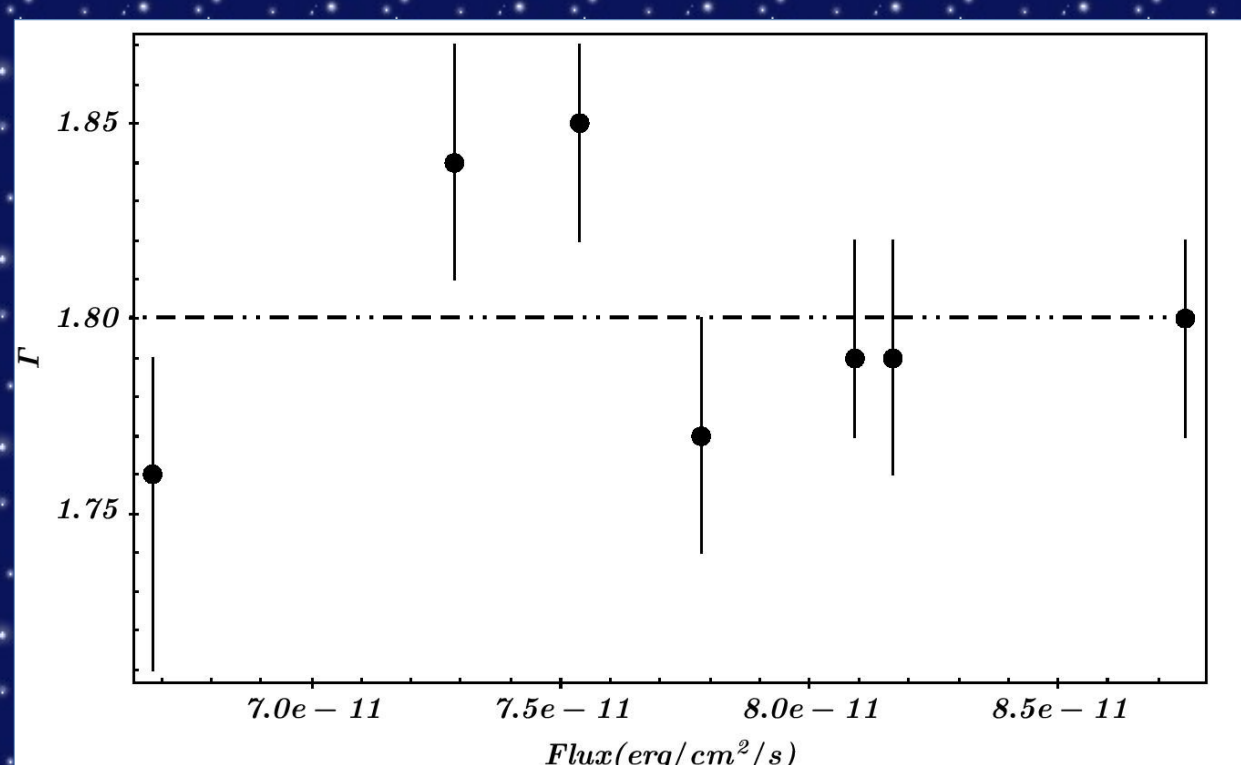


Fig. 6. Gamma as a function of the flux. The average value for Γ is 1.8.

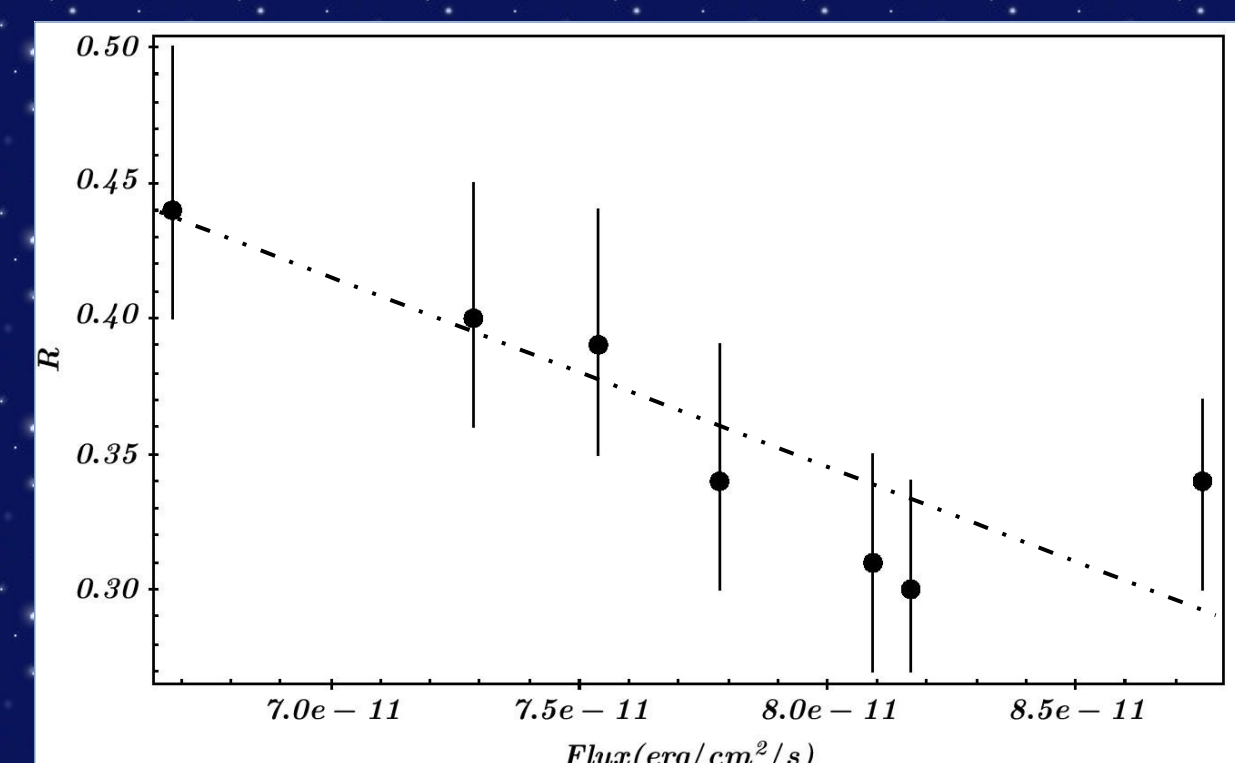


Fig. 8. Reflection versus flux in the 4-78 keV band.

Conclusions:

> We find large flux variability on ks time scales while modest flux variability occurs among the observations.

> A strong soft-excess component is found in all the observations and it extends up to 4 keV.

> From the XMM-Newton spectra we find FeK α and FeL γ lines.

> The neutral iron line is narrow and constant within all observations. This implies that during the campaign we observed reflection from distant gas.

> We are able to constrain the cut off energy with average value $E_{\text{cut-off}} \approx 220$ keV.

> Ongoing analysis will be focused on the broad band spectra and, in particular, on modeling the soft-excess component.